Journal of ASTM International, Vol. 8, No. 3
Paper ID JAI103286
Available online at www.astm.org

Akio Nishimoto,[1] *Kimiaki Nagatsuka,*[2] *Ryota Narita,*[2] *Hiroaki Nii,*[2] *and Katsuya Akamatsu*[1]

Effect of Gas Pressure on Active Screen Plasma Nitriding Response

ABSTRACT: An austenitic stainless steel AISI 304 was active screen plasma nitrided using a 304 steel screen to investigate the effect of the gas pressure on the nitriding response. The sample was treated for 18 ks at 723 K in 25 % N_2 + 75 % H_2. The gas pressure was changed to 100, 600, and 1200 Pa. The distance between the screen and the sample was also changed to 10, 30, and 50 mm. The nitrided samples were characterized by observing their appearance and surface roughness by optical microscopy, X-ray diffraction, and microhardness testing. After nitriding, polygonal particles with a normal distribution were observed at the center and edges of all the nitrided sample surfaces. The particles on the sample surface became finer with an increase in the gas pressure. The nitrided layer with a greater and homogeneous thickness was obtained at a low gas pressure of 100 Pa.

KEYWORDS: surface engineering, cathodic cage, edging effect, active screen plasma nitriding, stainless steel

Introduction

The nitriding process is widely used to improve the tribological properties and wear resistance of steels and titanium alloys. Compared with the conventional nitriding processes such as gas nitriding and salt bath nitriding, the glow discharge plasma nitriding process offers the following advantages: No pollution, high nitrogen potential, short treatment time, clean environment, and low energy consumption [1–3]. The components to be treated are subjected to a high cathodic potential to produce plasma directly on their surfaces. An "edging effect" occurs due to distortions of the electric field around the corners and edges of the components although the components are well heated. This results in nonuniformity in properties such as the hardness and thickness of the surface layer [4].

Recently, there has been considerable interest in active screen plasma nitriding (ASPN), through cage plasma nitriding, and cathodic cage plasma nitriding [5–19]. In these processes, the edging effect is completely eliminated because the plasma is produced on the cage and not directly on the samples [5]. These processes can be used to treat polymers that are nonconductive materials [7,11]. However, little information has been reported on the effect of the gas pressure on ASPN responses such as surface morphology, microstructure, and nitrogen depth.

In this study, austenitic stainless steel samples were nitrided by ASPN to investigate the effect of the gas pressure on ASPN responses.

Materials and Methods

The sample material used in this study was an austenitic stainless steel AISI 304 (chemical composition (mass %): 0.05 % C, 0.31 % Si, 1.63 % Mn, 0.04 % P, 0.03 % S, 18.60 % Cr, 8.00 % Ni, and balance Fe). The sample disk was 13 mm in diameter and 5 mm in thickness. The sample surface was mechanically ground with 150- to 1500-grit SiC, finely polished with 0.05 μm alumina in suspension, degreased ultrasonically in acetone, and dried in air before placing the sample in the nitriding furnace.

Manuscript received July 22, 2010; accepted for publication February 14, 2011; published online March 2011.
[1] Dept. of Chemistry and Materials Engineering, Kansai Univ., Osaka 564-8680, Japan.
[2] Graduate School of Science and Engineering, Kansai Univ., Osaka 564-8680, Japan.

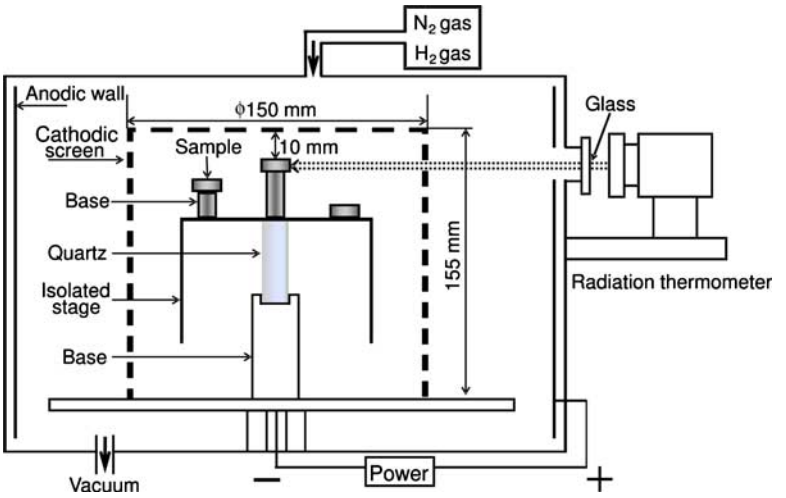

FIG. 1—*Schematic diagram of ASPN apparatus.*

ASPN experiments were carried out using a dc plasma nitriding unit (NDK, Inc., Japan, JIN-S1). Figure 1 shows a schematic diagram of the ASPN apparatus. A quartz (SiO_2) rod was placed on the cathodic stage in order to construct an isolated sample stage. The sample was placed on the sample stage in a floating potential and isolated from the cathodic screen and the anode. The screen, which was an expanded metal mesh of AISI 304 with a diameter of 150 mm and a height of 155 mm, was mounted on the cathodic stage around the sample stage. Mesh specifications of the expanded metal mesh used were L × S of 8 × 3 mm and a thickness of 0.5 mm. The AISI 304 rods were placed on the sample stage so that the distance between the screen and the sample could be changed to 10, 30, and 50 mm. The screen was thoroughly degreased ultrasonically in acetone.

Nitriding was performed in a nitrogen-hydrogen atmosphere with 25 % N_2+75 % H_2 for 18 ks at 723 K under 100, 600, and 1200 Pa by the ASPN process. After placing the sample on the sample stage, the chamber was evacuated at ~3 Pa. Then, nitrogen and hydrogen were introduced into the chamber and a dc bias voltage was supplied. After nitriding, the dc supply was switched off and the sample was cooled to room temperature in the furnace. The nitriding temperature was monitored using a radiation thermometer. The radiation thermometer was positioned at the sample in which the distance between the screen and the sample was 10 mm, as shown in Fig. 1.

After nitriding, cross sections of each sample were first cut using a low-speed saw and then polished and chemically etched. The nitrided microstructure was examined with a scanning electron microscope (SEM; JEOL, Japan, JSM-6060LV). The phase structures on the nitrided surface were determined by theta-2theta X-ray diffraction (XRD; RIGAKU, Japan, RINT-2550V) studies. A whole area of the top surface of nitrided samples was analyzed by XRD. In addition, the hardness of the surface and the cross sections of the nitrided sample were measured using a Vickers microhardness tester (Matsuzawa, Japan, MXT50) under a 0.1 N load. Seven indentations were performed on each sample and a 5 points average value except both maximum and minimum values was used for hardness.

Results and Discussion

After treatment, the appearance of the samples was examined visually. Edging effect was not observed in each sample. This shows that glow discharge did not occur on the sample surface because the sample was isolated by placing SiO_2 ceramics between the sample and the cathodic stage. Furthermore, in the ASPN process, the samples were heated to the treatment temperature by the heat radiated from the active screen, which promoted a higher homogeneity of temperature in the treated samples [4].

XRD results of the samples treated by the ASPN process are shown in Fig. 2. The γ-austenite and the S-phase, which is considered to be a supersaturated solid solution of nitrogen in the austenitic phase, were

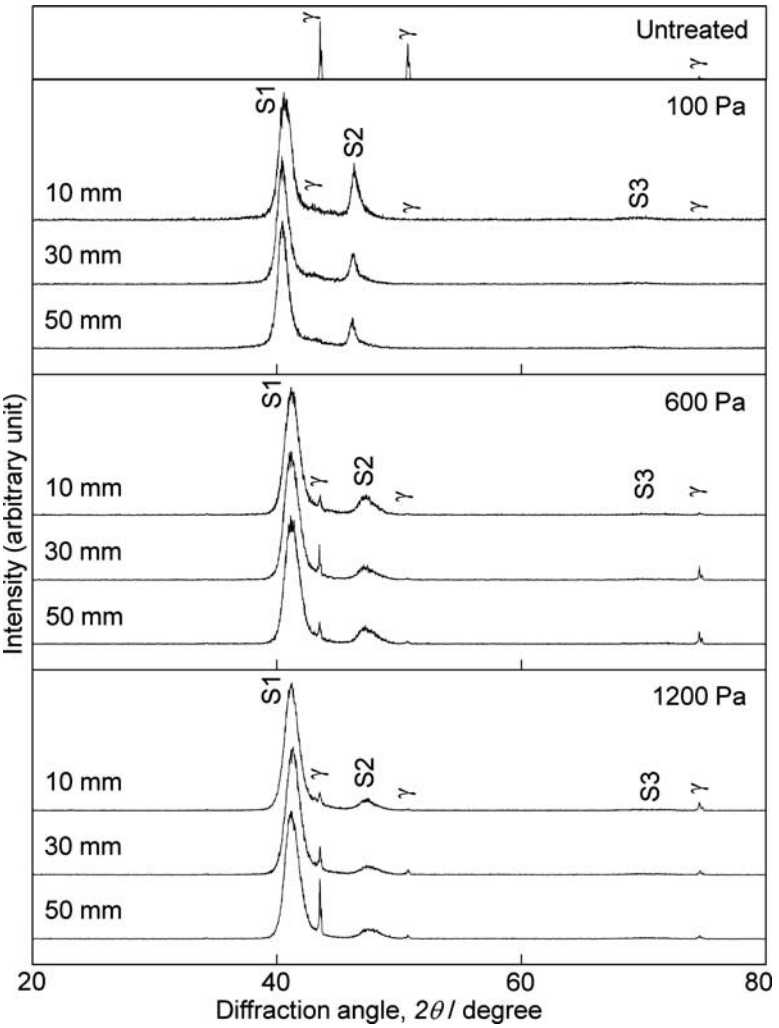

FIG. 2—*X-ray diffraction patterns of AISI 304 steel sample after ASPN at 723 K.*

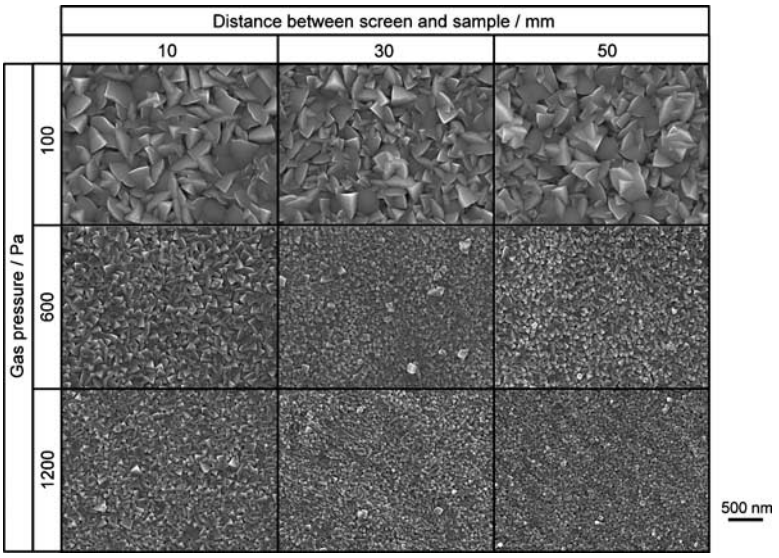

FIG. 3—*SEM micrographs of AISI 304 steel sample after ASPN at 723 K.*

TABLE 1—*Relationship between gas pressure and applied voltage.*

Gas pressure (Pa)	Applied voltage (V)
100	300–380
600	235–240
1200	240–245

identified on the sample surface in each condition. The layers formed on each sample were of the same phase irrespective of the gas pressure and the distance between the screen and the sample.

Figure 3 shows SEM micrographs of the sample surfaces treated by the ASPN process. The surface morphologies of samples treated at different pressures are different. Under the same gas pressure, a uniform normal distribution of polygonal particles was observed at the center and edges of the sample surface irrespective of the distance between the screen and the sample. The particle size becomes finer as the gas pressure increases. These results can be attributed to the Fe_xN particles present in the plasma; these particles were formed on the active screen and deposited on the sample surface during the ASPN process. Moreover, applied voltages during nitriding depended on gas pressures, as shown in Table 1. That is, applied voltages increased as the gas pressure decreased. At the lower pressure of 100 Pa, sputtered particles on the active screen increased because of the high voltage. Therefore, Fe_xN deposition increased as the gas pressure decreased, and these deposited particles grew.

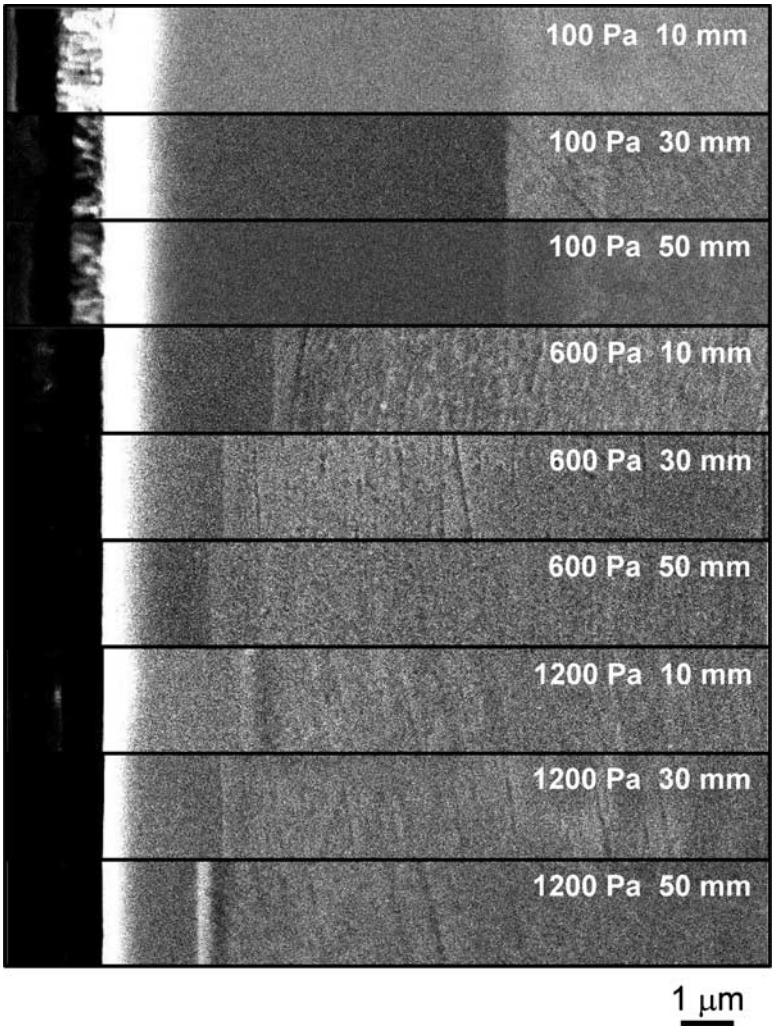

FIG. 4—*SEM micrographs of cross sections of AISI 304 steel sample after ASPN.*

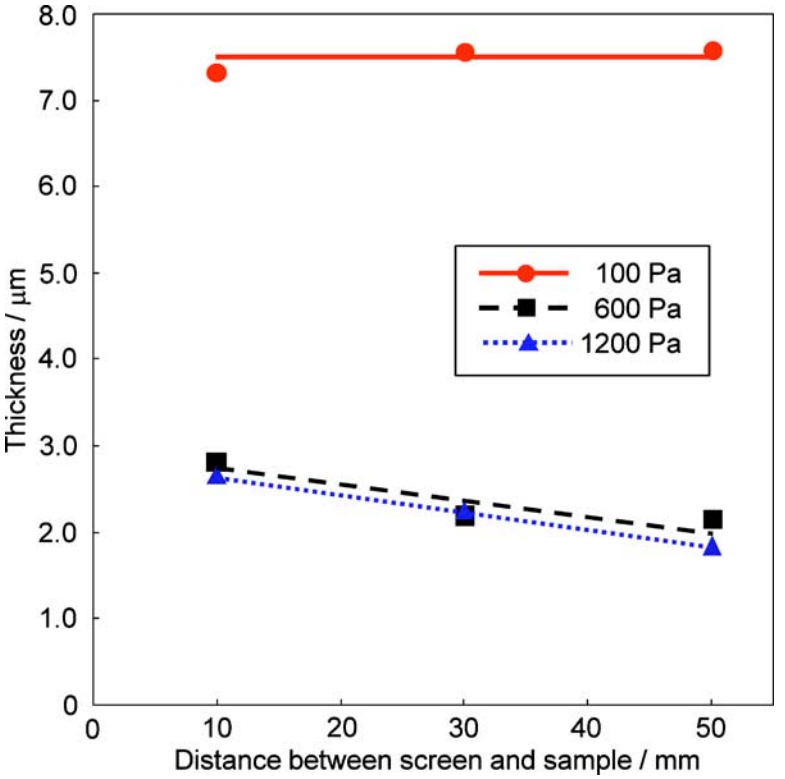

FIG. 5—*Effect of the gas pressure and the distance between the screen and the sample on the thickness of the nitrided layer after ASPN.*

The microstructures of the cross sections of the samples treated by the ASPN process are shown in Fig. 4. An S-phase layer that was very slightly corroded by oxalic acid was observed in the sample surfaces. Figure 5 shows the effect of the gas pressure and the distance between the screen and the sample on the thickness of the nitrided layer. When the samples were treated at 600 and 1200 Pa, the thickness of the nitrided layer decreased as the distance between the screen and the sample increased. This result indicates that the amount of the active species available for nitriding depends on the distance between the cathodic screen and the sample because the sample is isolated by placing SiO_2 ceramics between the sample and the stage. On the other hand, the nitrided layer treated at 100 Pa had a homogeneous thickness irrespective of the distance between the screen and the sample. Moreover, the thickness of the nitrided layer treated at 100 Pa was greater than those treated at 600 and 1200 Pa. These results suggest that the homogeneous temperature distribution expanded with a decrease of the gas pressure. As a result, the nitrided layer with a greater and homogeneous thickness was obtained at a low pressure of 100 Pa.

Figure 6 shows the cross-sectional hardness distribution of the samples treated by the ASPN process. The hardness decreased considerably toward the core of the substrate irrespective of the gas pressure and the distance between the screen and the sample. In addition, the hardening effect of the sample nitrided at 100 Pa was greater than those nitrided at 600 and 1200 Pa. The dependence of the distance on the surface hardness is a result of the thickness of the S-phase layer on the surface, as shown in Fig. 5.

Alves, Jr. et al. showed that the thickness of the nitrided layer depends on the sample geometry during the conventional dc plasma nitriding [4]. Jeong and Kim showed that the thickness of the nitriding layer and particle size on the surface increased with increasing gas pressure for the dc plasma nitriding [20]. In this investigation, the nitrided layer treated at a lower pressure of 100 Pa had a homogeneous thickness irrespective of the sample geometry and the distance between the screen and the sample. Moreover, the thickness of the nitrided layer treated at 100 Pa was greater than those treated at 600 and 1200 Pa.

Conclusions

Austenitic stainless steel AISI 304 samples were nitrided by the ASPN process using an austenitic stainless steel screen to investigate the effect of the gas pressure on the ASPN responses. After nitriding, polygonal

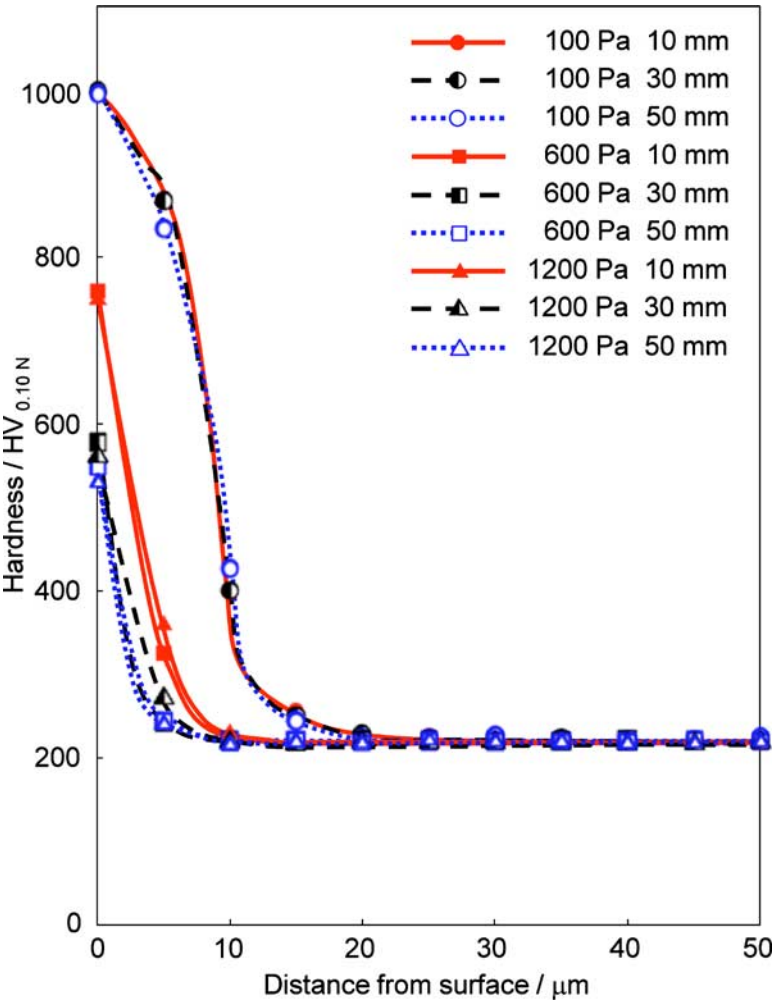

FIG. 6—*Hardness distribution of the cross sections of the AISI 304 steel sample after ASPN.*

particles with a normal distribution were observed at the center and edges of all the sample surfaces. Particles on the sample surfaces became finer as the gas pressure increased. Furthermore, under a gas pressure of 100 Pa, the thickness of the nitrided layer was almost the same irrespective of the distance between the screen and the sample. In contrast, the thickness of the nitrided layers under the gas pressures of 600 and 1200 Pa were smaller as the distance between the screen and the sample increased.

References

[1] Sun, Y. and Bell, T., "Plasma Surface Engineering of Low Alloy Steel," *Mater. Sci. Eng., A*, Vol. 140, 1991, pp. 419–434.

[2] Samandi, M., Shedden, B. A., Smith, D. I., Collins, G. A., Hutchings, R., and Tendys, J., "Microstructure, Corrosion and Tribological Behaviour of Plasma Immersion Ion-Implanted Austenitic Stainless Steel," *Surf. Coat. Technol.*, Vol. 59, 1993, pp. 261–266.

[3] Dong, H., "S-Phase Surface Engineering of Fe–Cr, Co–Cr and Ni–Cr Alloys," *Int. Mater. Rev.*, Vol. 55, 2010, pp. 65–98.

[4] Alves, C., Jr., da Silva, E. F., and Martinelli, A. E., "Effect of Workpiece Geometry on the Uniformity of Nitrided Layers," *Surf. Coat. Technol.*, Vol. 139, 2001, pp. 1–5.

[5] Li, C. X., Bell, T., and Dong, H., "A Study of Active Screen Plasma Nitriding," *Surf. Eng.*, Vol. 18, 2002, pp. 174–181.

[6] Li, C. X. and Bell, T., "Corrosion Properties of Active Screen Plasma Nitrided 316 Austenitic Stainless Steel," *Corros. Sci.*, Vol. 46, 2004, pp. 1527–1547.

[7] Li, C. X. and Bell, T., "Potential of Plasma Nitriding of Polymer for Improved Hardness and Wear

Resistance," *J. Mater. Process. Technol.*, Vol. 168, 2005, pp. 219–224.

[8] Hubbard, P., Dowey, S. J., Doyle, E. D., and Mcculloch, D. G., "Influence of Bias and In Situ Cleaning on Through Cage (TC) or Active Screen Plasma Nitrided (ASPN) Steels," *Surf. Eng.*, Vol. 22, 2006, pp. 243–247.

[9] Zhao, C., Li, C. X., Dong, H., and Bell, T., "Study on the Active Screen Plasma Nitriding and its Nitriding Mechanism," *Surf. Coat. Technol.*, Vol. 201, 2006, pp. 2320–2325.

[10] Alves, C., Jr., de Araujo, F. O., Ribeiro, K. J. B., da Costa, J. A. P., Sousa, R. R. M., and de Sousa, R. S., "Use of Cathodic Cage in Plasma Nitriding," *Surf. Coat. Technol.*, Vol. 201, 2006, pp. 2450–2454.

[11] Kauling, A. P., Soares, G. V., Figueroa, C. A., de Oliveira, R. V. B., Baumvol, I. J. R., Giacomelli, C., and Miotti, L., "Polypropylene Surface Modification by Active Screen Plasma Nitriding," *Mater. Sci. Eng., C*, Vol. 29, 2009, pp. 363–366.

[12] Nishimoto, A., Tokuda, A., and Akamatsu, K., "Effect of Through Cage on Active Screen Plasma Nitriding Properties," *Mater. Trans.*, Vol. 50, 2009, pp. 1169–1173.

[13] Gallo, S. C. and Dong, H., "Study of Active Screen Plasma Processing Conditions for Carburising and Nitriding Austenitic Stainless Steel," *Surf. Coat. Technol.*, Vol. 203, 2009, pp. 3669–3675.

[14] Nishimoto, A., Bell, T. E., and Bell, T., "Feasibility Study of Active Screen Plasma Nitriding of Titanium Alloy," *Surf. Eng.*, Vol. 26(1–2), 2010, pp. 74–79.

[15] Li, C. X., "Active Screen Plasma Nitriding–an Overview," *Surf. Eng.*, Vol. 26(1–2), 2010, pp. 135–141.

[16] Hubbard, P., Partridge, J. G., Doyle, E. D., Mcculloch, D. G., Taylor, M. B., and Dowey, S. J., "Investigation of Nitrogen Mass Transfer Within an Industrial Plasma Nitriding System I: The Role of Surface Deposits," *Surf. Coat. Technol.*, Vol. 204, 2010, pp. 1145–1150.

[17] Li, Y., Wang, L., Zhang, D., and Shen, L., "Influence of Bias Voltage on the Formation and Properties of Iron-Based Nitrides Produced by Plasma Nitriding," *J. Alloys Compd.*, Vol. 497, 2010, pp. 285–289.

[18] Dong, Y., Li, X., Sammons, R., and Dong, H., "The Generation of Wear-Resistant Antimicrobial Stainless Steel Surfaces by Active Screen Plasma Alloying with N and Nanocrystalline," *J. Biomed. Mater. Res., Part B: Appl. Biomater.*, Vol. 93B, 2010, pp. 185–193.

[19] Nishimoto, A., Nagatsuka, K., Narita, R., Nii, H., and Akamatsu, K., "Effect of the Distance Between Screen and Sample on Active Screen Plasma Nitriding Properties," *Surf. Coat. Technol.*, Vol. 205, 2010, pp. S365–S368.

[20] Jeong, B. Y. and Kim, M. H., "Effects of the Process Parameters on the Layer Formation Behavior of Plasma Nitrided Steels," *Surf. Coat. Technol.*, Vol. 141, 2001, pp. 182–186.